

Title: **Beam-mode model of FTS.**

Prepared by: Martin Caldwell

**Summary.**

This FTS model uses a single-mode beam throughout (hence aberrations are not included), and is based on design bolsp460b. We calculate beam patterns at the detector + fringe visibility.

At the maximum +Y off-axis angle of 1 arcmin, and an exaggerated rooftop displacement of 10cm (OPD=40cm), the reduction in fringe visibility due to lateral pupil shift is 56 % relative to the zero-OPD case. The figure for SPIRE's travel of 31.25mm (OPD=125mm) is 85%.

**Beam model.**

A single mode (gaussian) unpolarised beam is traced forwards through the system. The input beam waist is positioned at the system entrance pupil, and its waist size is set to a 1/e amplitude edge taper at the pupil. The wavelength used is 0.5mm and the input beam pattern is shown in fig.1.

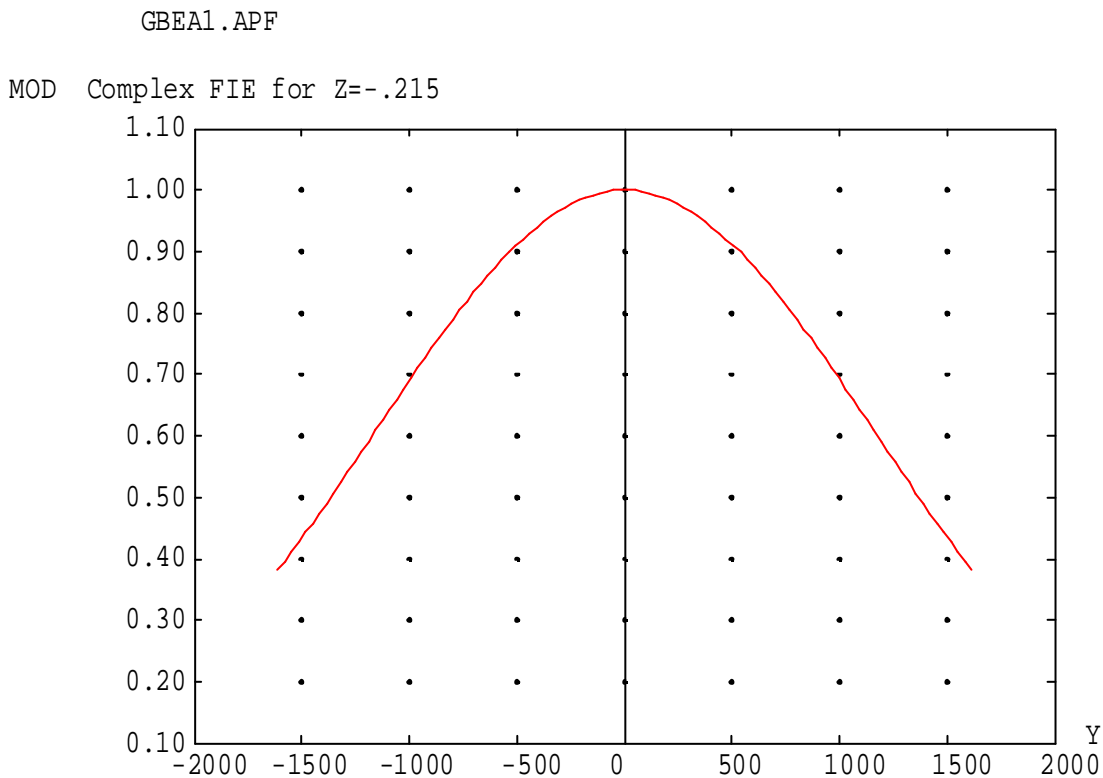


Fig.1. Input beam Modulus plotted over system entrance pupil. (horiz. Dim'n = mm).

Title: **Beam-mode model of FTS.**  
Prepared by: Martin Caldwell

In this 1<sup>st</sup>-cut the beam is propagated as a single mode, i.e. using one ASAP beam. Consequently at all points the beam is a full gaussian, and so the edge-clipping implied by fig.1. is not applied. ASAP maps the mode using a base ray (running along the mode centre) plus several 'parabasal' rays. In the ray-trace diagrams here only the base ray is plotted:-

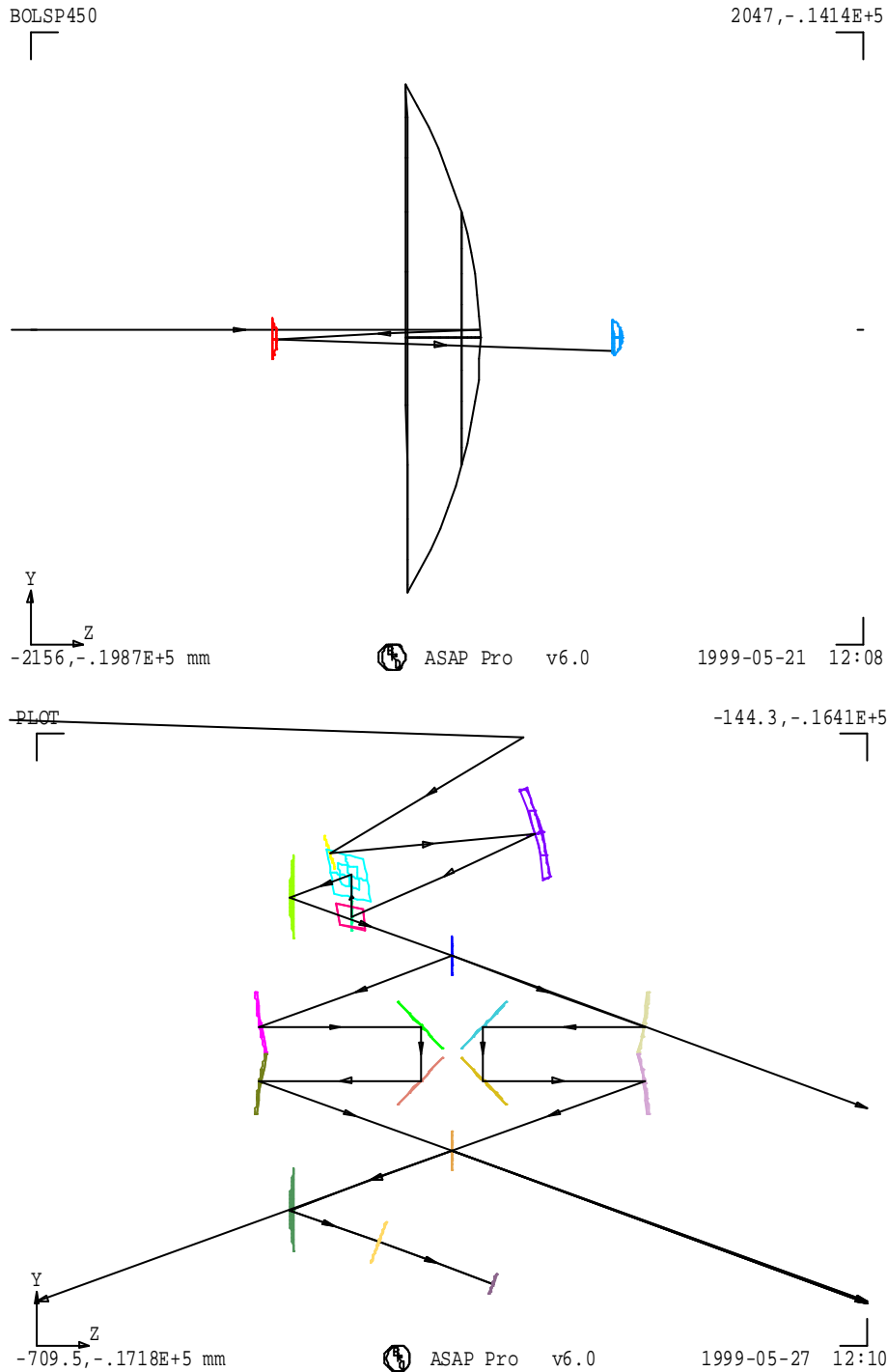


Fig.2. Propagation through telescope & instrument.

**Title: Beam-mode model of FTS.**

Prepared by: Martin Caldwell

In the present model the mode is amplitude-split at the 1<sup>st</sup> beamsplitter, generating 2 beams, these are again split at the 2<sup>nd</sup> beamsplitter, so that 2 beams, each having 1/4 of the input power, arrive at the detector.

### Single-arm pattern.

The beam pattern from one arm at the detector is shown in fig.3.

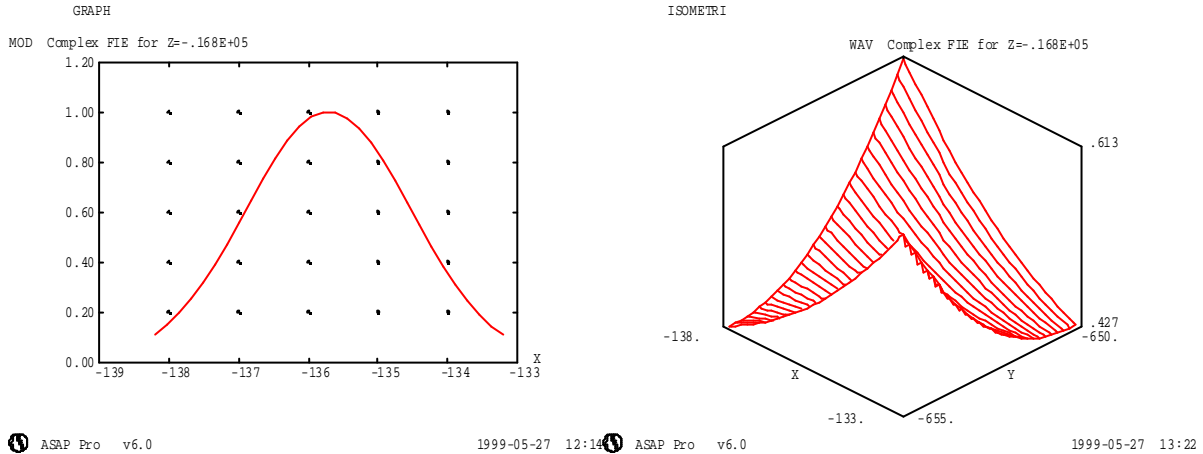


Fig.3. Single-beam pattern at detector. Modulus at left, wavefront (in number of waves) at right.

From this pattern the 1/e amplitude point is measured to be 1.75mm, as compared to the expected value of (f/5 beam) (N-0006.3).

$$W = (2/\pi).F\lambda$$

$$= 1.59 \text{ mm}$$

At this location the beam should have a waist & so the wavefront should be flat. Therefore the saddle shape actually found indicates some limitation in the method. The single mode pattern was also checked at distances + & - 4mm from the detector (fig.4).

**Title: Beam-mode model of FTS.**

Prepared by: Martin Caldwell

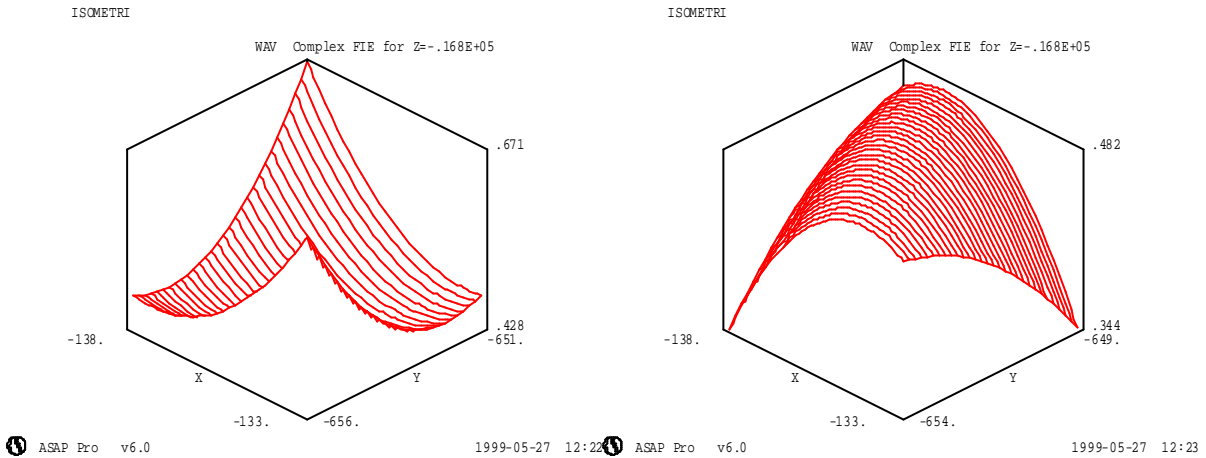


Fig.4. Wavefront at  $-4\text{mm}$  (left) and  $+4\text{mm}$  (right).

This shows that the beam waist is near the geometric optics (GO) focal plane (detector), as it has opposite curvatures either side of this plane.

The distorted wavefront near focus is not a measure of aberrations since a single mode does not sample the components' forms. Instead it is due to paraxial approximations used in the ASAP ray-trace, whereby the mode's waist & divergence rays are assumed to be paraxial with the base ray. To test this computations were made for telescope alone, with the beam on-axis (aberration-free system). In this case, at  $\lambda=1\text{mm}$ , the beam waist was found to be  $\Delta=-1\text{mm}$  from the GO focus, and flat to  $< 10^{-4}$  waves. This shows that the ASAP single mode model behaves well only in the absence of aberrations.

In order to map aberrations, it is necessary to use a grid of ASAP modes to map the beam, and this will also necessarily mean that edge-clipping is included.

A repeat of the above off-axis analysis using an array of  $11 \times 11$  beams gives a flatter wavefront than in fig.3 showing that the use of grid is more accurate than that of a single mode. However, for reasons of simplicity & speed (see below) we only use the single-mode in this note.

**Title: Beam-mode model of FTS.**  
 Prepared by: Martin Caldwell

**Long-wave defocus effects.**

From mode theory the long-wave beam waist is expected to be displaced from the geometric focus. In the above system the calculation of this effect (other than via the model itself) is complicated by the many imaging stages and folds in the beam.

As an example however, we consider the effect of the telescope alone in the  $\lambda=1\text{mm}$  test case above : The focal plane is a distance  $z\sim 2370\text{mm}$  from M2. At short-wave this distance is equal to the wavefront ROC at the mirror. At long wavelength it is a shorter distance  $z$  given by the inverse of :

$$\text{ROC} = z(1+(z_0/z)^2)$$

Where  $\text{ROC}=2370\text{mm}$ ,  $z_0=\pi \cdot w_0^2/\lambda=92\text{mm}$ . This gives  $z=2366.4\text{mm}$ , i.e. the waist should be displaced by  $\Delta=-3.6\text{mm}$  from GO focus. The analysis gives  $-1\text{mm}$ , and this discrepancy needs further investigation.

In the equal-arms symmetric position (fig.2), the pattern due to each beam is identical, but if we scan the FTS to an asymmetric position, as shown in fig.5, the above effect should appear differently in each beam at the detector as they have travelled different path lengths (the finite diffraction-limited divergence of the beam leads to differing wavefront curvatures in each arm)

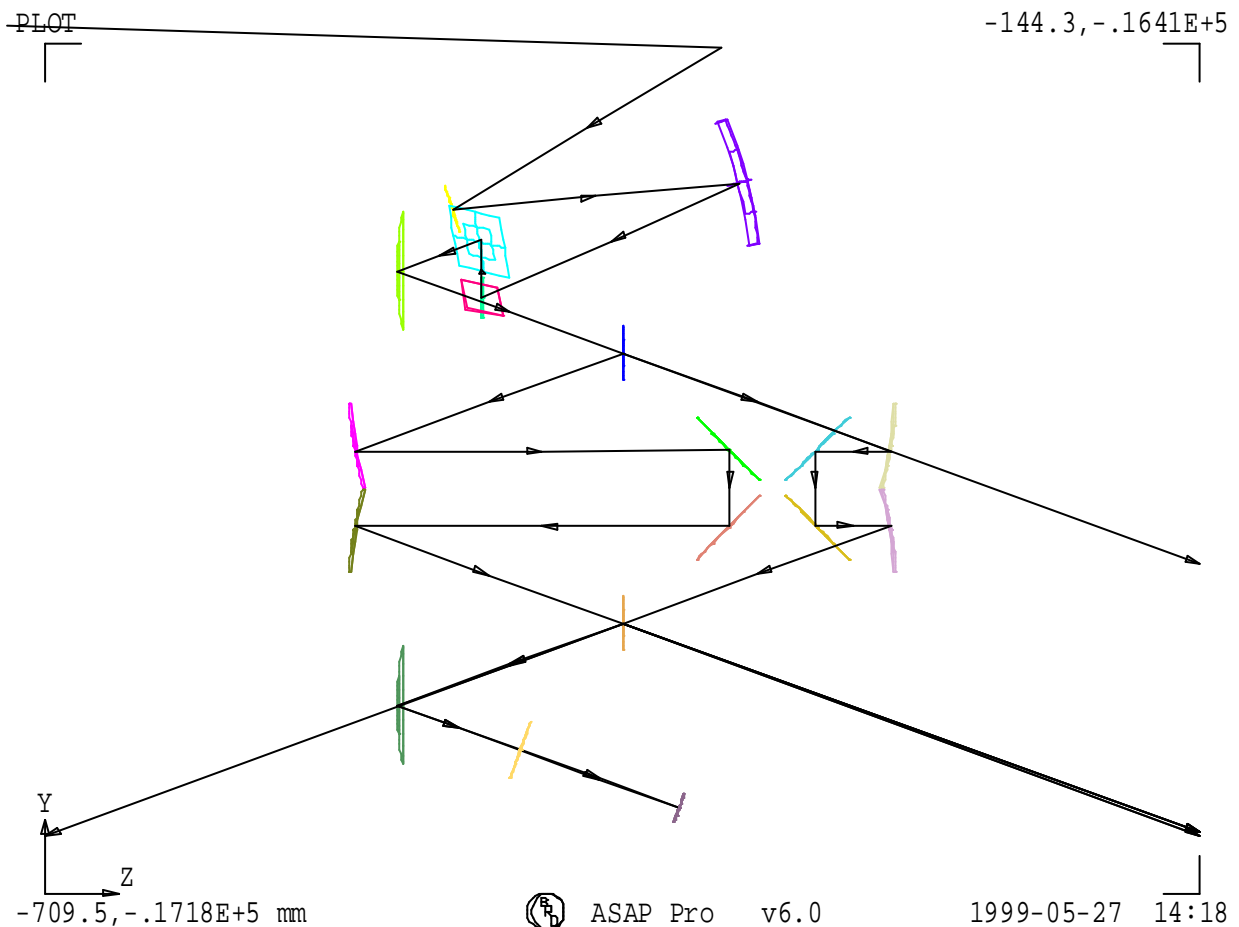


Fig.5. FTS with rooftop moved to left by  $\Delta z=100\text{mm}$  (gives  $\text{OPD}=8$ .  $\Delta z$ )

In the short-wavelength case this effect would be absent, since the beam is collimated in the changed section of the system. The patterns due to each beam are shown in fig.6, where we see that in comparison to the equal-arm pattern of fig.3., each arm is now defocused (I.e, has added curvature) in the opposite sense in each case.

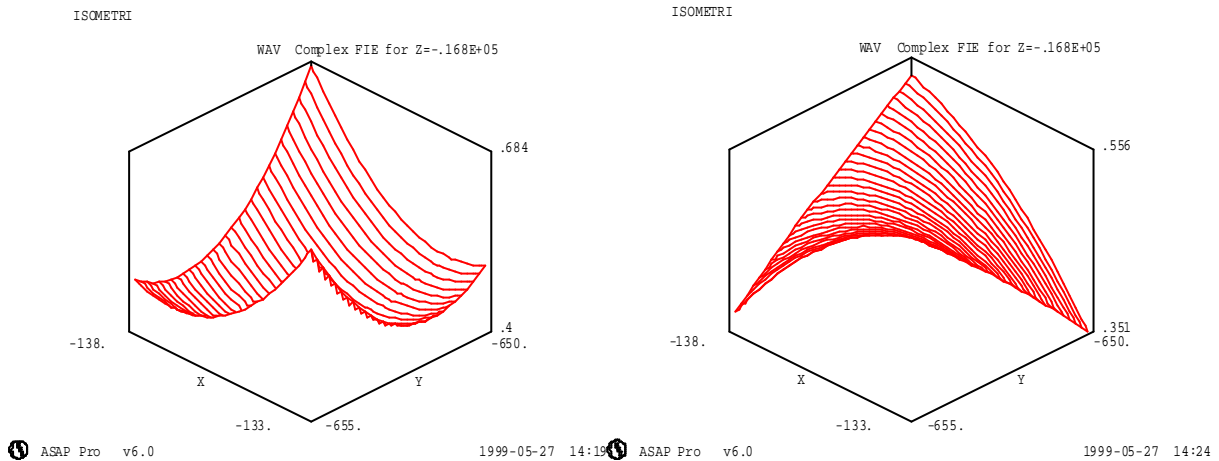


Fig.6. Single-beam patterns in each arm, at left is longer arm (+OPD), at right is shorter (-OPD).

The effect of this on fringe visibility is that of diffraction-limited apodisation, (calculable analytically). The present model could be used to further verify this effect, but first the accuracy (# or rays) would have to be increased.

### Interferometry.

Due to the common path & symmetry of the system, the beam entering each arm has a similar shape, and so the FTS signal should not be affected by the limited accuracy of the single-beam pattern.

We therefore can use the single-mode model to study the effect of FOV-induced pupil wander over the travel range of the FTS.

To see this effect we trace the mode at an off axis angle of 1 arcmin in the +Y direction, at an exaggerated OPD position, as shown in fig.7.

<b>FIRST - SPIRE</b>	<b>DocNo:</b> <b>SPIRE/RAL/NOT/000269</b>
<b>Title: Beam-mode model of FTS.</b>	<b>Issue: 2</b>
Prepared by: Martin Caldwell	<b>Date: 19-06-00</b>

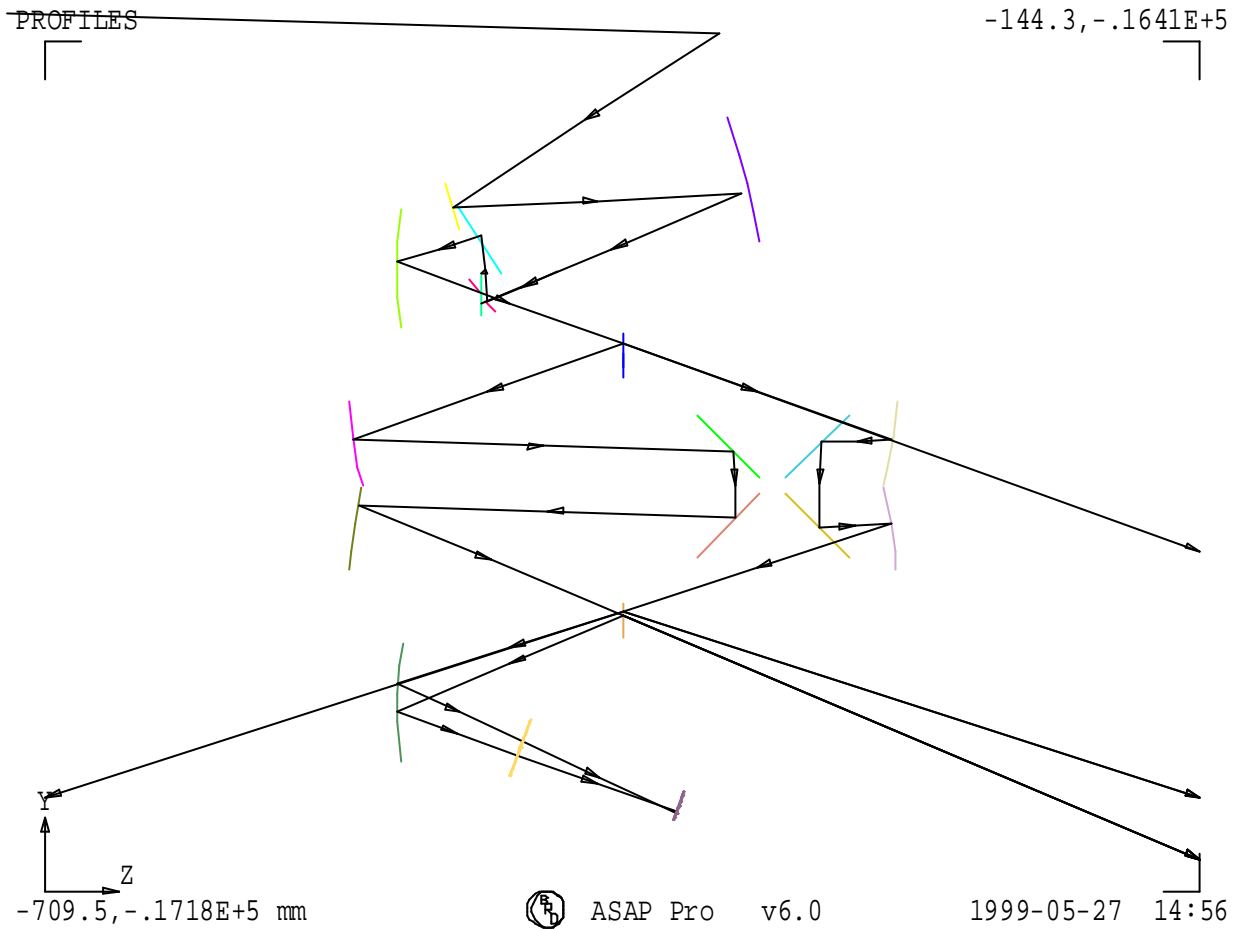


Fig.7. Beam paths at +Y extreme of FOV, exaggerated mirror travel  $\Delta Z=100\text{mm}$ .

Here the re-combined beams are displaced, mainly in Y, by 0.38mm, and have Y-direction cosines of  $-0.422$  &  $-0.342$ .

To model the FTS functions the two-beam pattern total (i.e. detected) energy is calculated, whilst scanning the roof-top position. An example two-arm pattern is shown in fig.8, and example scans are shown in fig.9.

**Title: Beam-mode model of FTS.**  
 Prepared by: Martin Caldwell

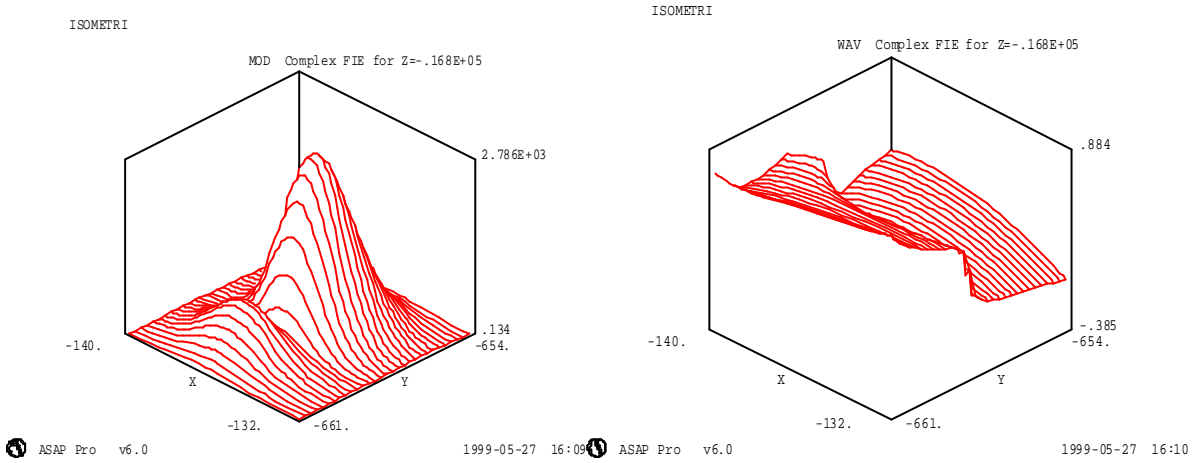


Fig.8. Example 2-arm pattern (case of max. OPD, & near destructive interference). Left=Modulus, Right=wavefront.

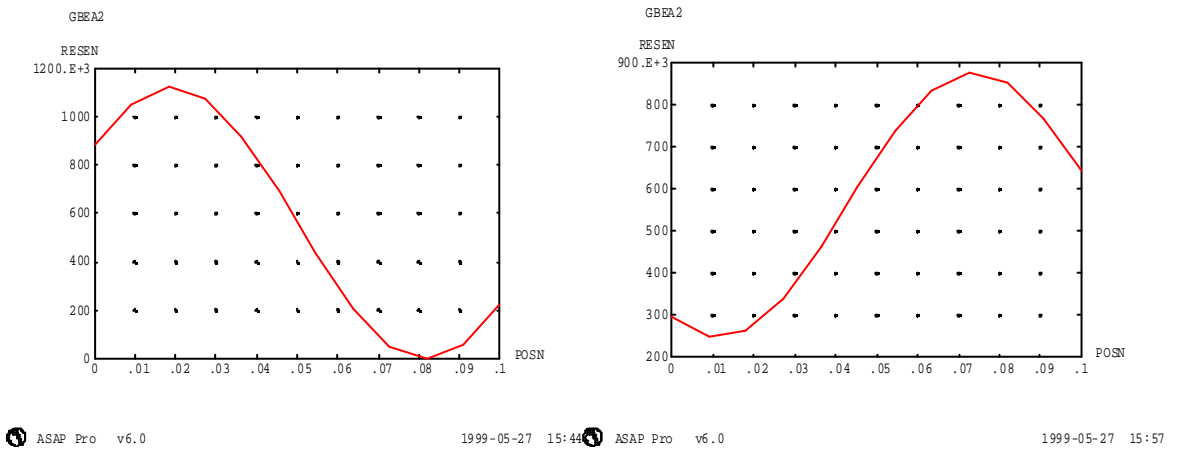


Fig.9. FTS 1/2-wave scan (detector energy vs rooftop position), for +Y FOV, Left: near OPD=0, Right: near OPD=4\*100mm.

Fringe visibility or contrast is:

$$\gamma = \text{fringe amplitude/mean amplitude level}$$

$$= 620/1100 = 56\%.$$

The actual travel in SPIRE is 31.25mm rather than 100 mm, for which the contrast is 85 %.